Operation of Networked Microgrids in a Distribution System

Fan Zhang, *Student Member, IEEE*, Huiying Zhao, *Student Member, IEEE*, and Mingguo Hong, *Member, IEEE*

***Abstract*—In this work, a PSCAD electromagnetic model is constructed for a microgrid community. It consists of three microgrids networked through the medium voltage (MV) distribution system as a practical case of the distributed resource island systems of IEEE Standard 1547.4. Typical operational scenarios are then simulated for both grid connected and islanded mode of operation. The study outcomes demonstrate the operational feasibility of networked microgrids in electrical distribution systems and the effectiveness of common droop controls in facilitating energy transaction of the microgrids and maintaining voltage and frequency stabilities under normal network disturbances. This investigation is significant in that it addresses the needs and issues arising from primary controls for facilitating the energy transactions of secondary and tertiary controls in the hierarchical control strategy of networked microgrids in the MV distribution system. Future studies of the secondary and tertiary control algorithms will need to incorporate new requirements for ensuring distribution system voltage and frequency securities.**

***Index Terms*—Distributed generation, distribution system, hierarchical controls, microgrid community, network microgrids, renewable generation.**

I. INTRODUCTION

In recent years, microgrids have been recognized among academia, industry, and government as an important means to integrate distributed generation, achieve energy security, and improve grid resilience [1]–[3]. According to the definition by U.S. Department of Energy, a microgrid is "a group of interconnected loads and distributed energy resources within clearly defined electrical boundaries that acts as a single controllable entity with respect to the grid" [4]. The key features of microgrids include the ability to operate in both grid-connected and islanded modes, and the integration of renewable generation. Broader views of microgrids can be found in research literature where the boundaries of microgrids are flexibly defined [5], [6]. According to the IEEE Standard 1547.4 [6], a hierarchy of various capacity scale microgrids can be constructed within the electrical distribution system, ranging from facility microgrids that mainly involve the LV network of energy end user to feeder microgrids and substation microgrids that include portions of the medium voltage (MV) distribution system network (Fig. 1). Microgrids are expected to fulfill a number of operational and economic benefits, such as performing network ancillary services, providing power during grid outage, and participation in the electricity market [1], [7]. So far, real world microgrids have been built for technology demonstration providing services to critical loads [8], [9]. The further proliferation of microgrids in electrical distribution systems, however, is still awaiting improved cost benefits, establishing better business cases for the electrical utility companies, and regulatory policy changes.

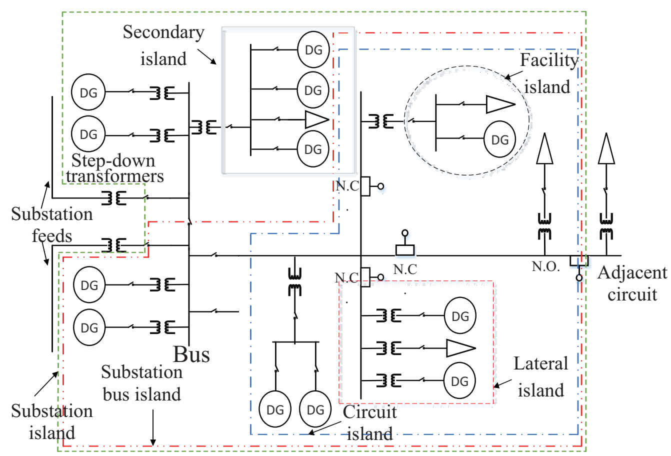

Fig. 1. Example of a DR system island [6].

At the same time, microgrids continue to attract interest among researchers in academia. Numerous studies have been conducted that focus on the coordinated control strategies of microgrid operation. A general control framework is a coordinated three-layer hierarchical structure [10] where the fast response primary controls ensure power quality through frequency and voltage regulation; the slower response secondary controls adjust setpoints of the primary controls to maintain power balance on short terms; and tertiary controls schedule the secondary control setpoints on longer terms to ensure energy adequacy and economic operation. Typically, primary controls are implemented locally with droop characteristics, and the secondary and tertiary controls are implemented centrally. Due to the special system characteristics of microgrids, some primary control schemes also engage in site-to-site communication to improve power-sharing performance.

Manuscript received July 10, 2015; revised November 1, 2015; accepted November 23, 2015. Date of publication December 30, 2015; date of current version December 18, 2015.

F. Zhang, H. Zhao, and M. Hong (corresponding author) are with the Electrical Engineering and Computer Science department of the Case Western Reserve University, Cleveland, OH 44106, USA (e-mails: fan.zhang@case.edu, huiying.zhao@case.edu, mingguo.hong@case.edu).

Digital Object Identifier 10.17775/CSEEJPES.2015.00043

To reduce dependency on communication links and improve reliability, the trend of research studies is to employ decentralized or distributed strategies for the control of all three layers [11], [12].

Networked microgrids or microgrid communities, defined as the aggregation of interconnected microgrids, on the other hand, have been of considerable interest [13]–[15]. These studies focus on both power sharing strategies and energy management under a simplified physical assumption of the microgrids sharing a common AC bus. In reality, microgrids are most likely interconnected through the MV distribution system network, as discussed in [6].

The impacts of the distribution network on the dynamic interactions among the microgrids during as well as on voltage regulation must be understood and managed for distribution system steady-state operation. In addition, the lower level (primary and secondary) controls that facilitate energy transaction among the microgrids need to be identified and validated.

So far, research studies on microgrid communities as a group of networked microgrids have been mostly concerned with optimal energy transaction strategies to meet economic objectives. Static and dynamic securities of the MV distribution system under normal conditions and during network events have not been adequately evaluated. Perhaps the most relevant works found in the research literature are [16], [17], in which the dynamic performance of the distribution system as a single microgrid was studied under various operating conditions.

This paper studies a microgrid community that involves the MV distribution system network and three facility microgrids constructed based on an existing low voltage (LV) distribution system network: a building, a remote community, and a small factory. Along with a section on MV distribution system network, the interconnected microgrids form a feeder microgrid in the sense of [6]. A detailed electromagnetic model has been constructed in PSCAD [18] for the microgrid community that contains a rich mix of conventional (1.5 MW), renewable (0.9 MW), and energy storage resources (0.5 MW). Hierarchical control strategies are assumed for power and energy management both at the individual microgrid level and at the microgrid community level. Therefore, energy management systems with the necessary sensing and control infrastructure are present at both levels as well. This study, however, does not specify the actual secondary and tertiary control algorithms that lead to setpoint decisions for primary controls. Efforts will primarily focus on investigating the dynamic stabilities of voltage and frequency of the microgrid community where the fast-response local controls of DERs react to both abrupt operating condition changes and ramped setpoint adjustments. Using extensive electromagnetic simulations of operational scenarios, this study validates 1) the operational feasibility of the microgrid community under both steady-state and dynamic conditions, and 2) effectiveness of a primary control strategy that mainly consists of common droop controls in facilitating energy transactions of microgrids entities while maintaining overall system voltage and frequency securities.

II. The Microgrid Community Model

A. The Distribution System Network Model

The MV distribution system model in this study is the IEEE 34 Node Test Feeder [19]. As shown in Fig. 2(a), this test system represents an actual 24.9 kV distribution system network in the U.S. state of Arizona, featuring long

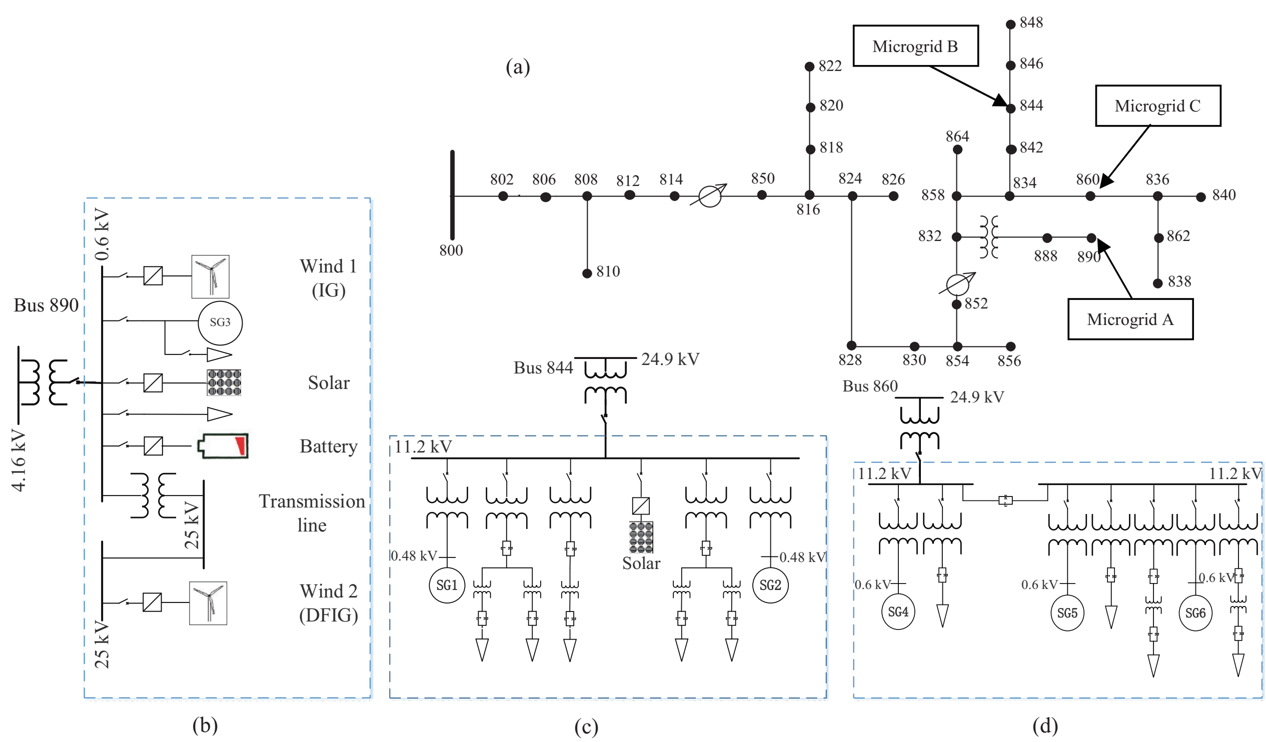

Fig. 2. A microgrid community with 3 microgrids. (a) IEEE 34 Node Distribution System. (b) Microgrid A. (c) Microgrid B. (d) Microgrid C.

feeders with light, distributed, and unbalanced loads. The point of common coupling (PCC) of the microgrid community is located at node 832. This study modifies the IEEE 34 Node Test Feeder model by adding three microgrids downstream from the PCC, each at nodes 890, 844 and 860, respectively. These nodal locations are selected so that the capacities of the microgrids can be adequately rated to serve the majority of the loads in the microgrid community. At the same time, the distances among the microgrids are far enough for studying voltage regulation. The characteristics of the three microgrids are described in the following.

B. Three Microgrids

1) Microgrid A: As shown in Fig. 2(b), this microgrid represents one that serves a remote community with a natural gas synchronous generating units, two wind generating units [a doubly fed induction generator (DFIG) and an induction generator (IG)], a solar PV generating unit, and a battery energy storage (BESS) unit.

1) Synchronous generator (250 kW). This is implemented with real power frequency (P-f) turbine governor droop control and the reactive power voltage (Q-V) droop control for the rotor excitation circuit. A generator can be placed on the voltage regulation mode to regulate the terminal voltage against a target setpoint through reactive power injection. The control circuit diagram is shown in Fig. 3(a).
2) Solar PV generating unit (210 kW). The solar PV generation unit is placed on maximum power point tracking (MPPT, Fig. 3(c)) and interfaces with the rest of the microgrid through a DC/AC invertor, as shown in Fig. 3(d).
3) IG (200 kW) and DFIG (60 kW) wind generating units. Both are on MPPT.
4) BESS (500 kW). The BESS interfaces with the rest of the microgrid through a 4-quadrant inverter. It is on P-Q control, as shown in Fig. 3(b).
5) Loads. All loads are modeled as composited constant power, constant current, and constant impedance types (ZIP). The amount of critical load is 160 kW.

2) Microgrid B: As shown in Fig. 2(c), this microgrid represents one that serves a commercial building with over 800 kW onsite generation capacity including two natural gas synchronous generating units (200 kW each), and a solar PV (460 kW). The local control schemes for the synchronous generators and the solar PV are similar to those of Fig. 3(a), Fig. 3(c) and Fig. 3(d). All loads are ZIP types. The amount of critical load is 260 kW.

3) Microgrid C: As shown in Fig. 2(d), this microgrid represents one that serves a manufacturing plant with onsite co-generation (such as combined heat and power type). Three natural gas synchronous generating units (250 kW each) are equipped with similar turbine governor and excitation controls as in the microgrid A. All loads are modeled as ZIP types. The amount of critical load is 140 kW.

C. Hierarchical Controls

The hierarchical controls are essential for supporting the microgrid community operation. In the hierarchical control

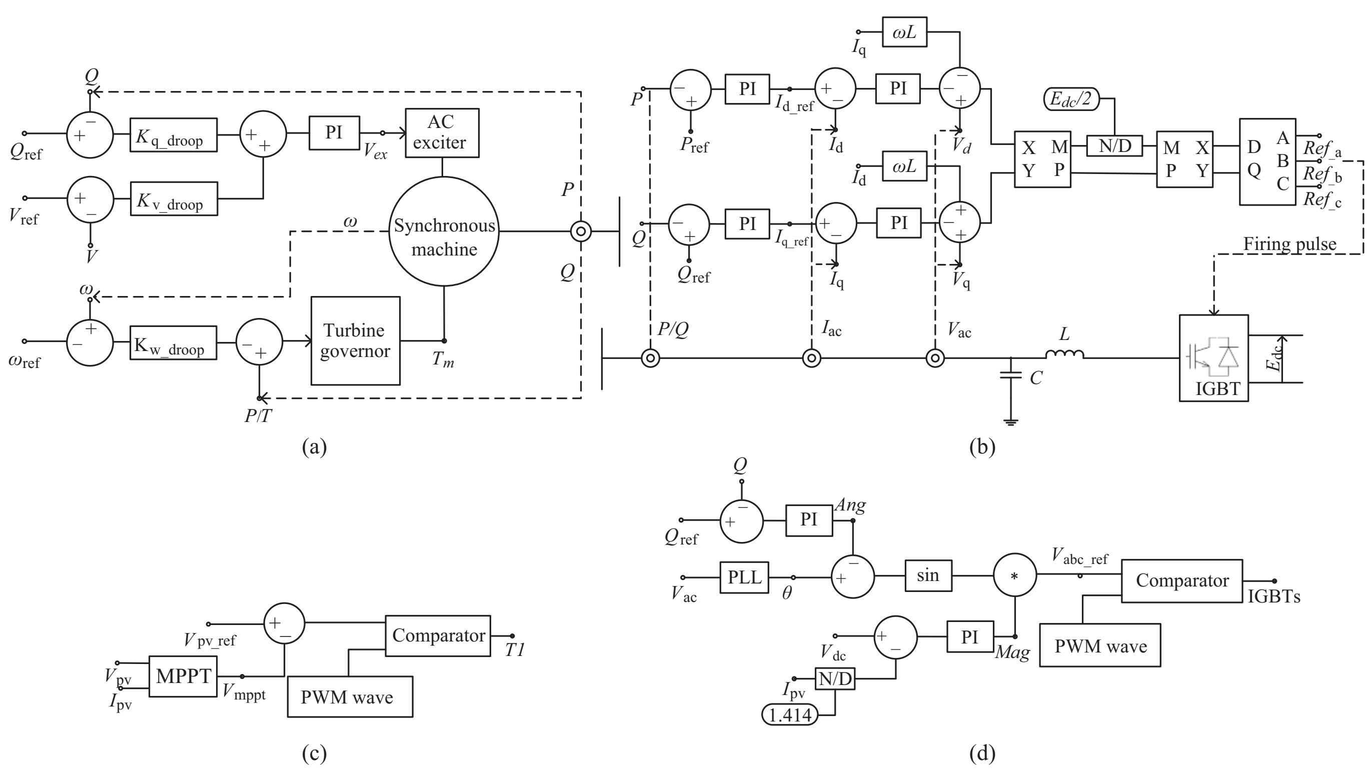

Fig. 3. Selected local control schemes for synchronous generator, solar PV and BESS inverter. (a) Synchronous generator P-f and Q-V droop controls. (b) Current decoupled control of BESS inverter VSC. (c) MPPT of Solar PV. (d) DC/AC PV Inverter.

structure, the primary controls are mainly implemented as local controls for the physical devices. As proposed in most microgrid community studies, two levels of controls are typically designed for the secondary controls, one at the microgrid level and another at the microgrid community level. Similarly, two levels of tertiary controls can be present, one at the microgrid level and another at the microgrid community level.

1) Primary Controls: The primary controls refer to all the local controls described in section II. B, including frequency and voltage droop controls (P-f/Q-V) for the synchronous generators, four-quadrant P-Q controls for the BESS units, and MPPT controls for the solar and wind units. These represent the most common primary control methods that are currently applied in distributed generation technology.

2) Secondary and Tertiary Controls: The secondary controls are implemented at both the microgrid and microgrid community levels. The secondary control function at the microgrid is performed by the microgrid Energy Management System (M-EMS). The microgrid can be placed on the active power and voltage regulation mode, i.e., the P-V mode, or on the active and reactive power regulation mode, i.e. the P-Q mode. In the P-V mode, the microgrid secondary control dispatches the active and reactive powers of the generation resources in the microgrid to follow scheduled active power interchange and voltage setpoints (P_{ref}, V_{ref}) measured at the microgrid PCC. In the P-Q mode, the microgrid secondary control dispatches the generation resources to follow the scheduled active and reactive power interchange setpoints (P_{ref}, Q_{ref}) measured at the PCC. All setpoint schedules are provided by the higher level microgrid EMS (MC-EMS).

There are many proposed algorithms that perform energy transaction scheduling (secondary and tertiary controls) to achieve optimal economic objectives. Centralized, decentralized, or distributed secondary control schemes can be implemented at the microgrid community level in MC-EMS to compute and communicate setpoints (P_{ref}, Q_{ref}, V_{ref}) to the individual microgrids. Procurement and deployment of operating reserves on DER to respond to either frequency or voltage events in the grid system will also become important requirements for power system operational security. Each microgrid will carry operating reserves of active and reactive power requirements (P_{res}, Q_{res}). The active and reactive power operating reserves will be procured and deployed through instructions from the MC-EMS.

The secondary and tertiary controls will not be elaborated in greater detail here, as the focus of this study is to identify the effectiveness of primary controls in enabling the energy transaction schedules of the secondary and tertiary controls.

III. Grid Connected Operation

In this case study, the distribution system is energized at the substation and the microgrid community is in grid-connected mode of operation. All microgrids within the microgrid community are placed in P-Q control mode where the active and reactive power setpoints (P_{ref}, Q_{ref}) for each microgrid are provided by the MC-EMS. The M-EMS in turn places its dispatchable generation resources on the P-Q control mode, and through economic dispatch within the microgrid (as a secondary control function), regulates the power interchanges at the microgrid PCC to follow setpoints (P_{ref}, Q_{ref}).

The objectives of the economic dispatch algorithms for both the microgrids and microgrid community are to minimize operational costs while maintaining the bus voltages and branch (lines and transformers) flows within security limits. Economic dispatch functions at both levels may be performed at such a periodicity as to help to meet both economic objectives and network security requirements. Additionally, at the microgrid community level, economic dispatch can leverage the microgrids as resources to fulfill important network operational objectives such as distribution system voltage regulation and conservation voltage reduction (CVR), along with other available controls in the distribution system such as automatic voltage regulators (AVR) and capacitor banks.

The following simulation cases evaluate the impact of economic dispatch on the system stability and power quality while the microgrid community is in grid-connected mode of operation. One key study objective is to evaluate network voltage and frequency stabilities when the generator active power setpoints are drastically increased from low to high output levels. In a MV distribution system network where R/X ratio is high, this may potentially lead to voltage instability.

A. Economic Dispatch of Active Power

In this case study, a series of adjustments are made to the active power setpoints of synchronous generators and BESS units along with abrupt load changes without additional reactive power dispatch for voltage support. Meanwhile, power, voltage and current measurements are taken at key nodal locations.

1) Microgrid Community: The microgrid community was initially in steady-state operation with all DERs connected online and supplying power. The series of generation setpoint and load changes are recorded in Table I. The power interchange at PCC (i.e., node 832) as a function of time is shown in Fig. 4(a), where the microgrid community moved from initially importing 200 kW at $t = 10$ s to finally exporting 120 kW at $t = 65$ s. The PCC voltage measurement and microgrid community frequency are shown in Fig. 4(b) and Fig. 4(c) respectively. Samples of the steady-state three phase voltage

TABLE I
Active Power Setpoints and Load Adjustments

T (s)	Device	ΔP, ΔQ	T (s)	Device	ΔP, ΔQ
15	BESS	+100 kW	39	L_890	+30 kW
22	BESS	+400 kVar	39	SG5	+15 kW
26	L_890	+24 kVA	39	SG6	+15 kW
26	SG1	+12 kW	43	SG4	+15 kW
26	SG2	+12 kW	46	SG4	+20 kW
28	L_890	+24 kVA	50	BESS	+50 kW
29	SG1	+12 kW	51	SG5	+15 kW
29	SG2	+12 kW	51	SG6	+15 kW
31.5	L_890	+32 kW	53	SG5	+20 kW
32	SG1	+16 kW	53	SG6	+20 kW
32	SG2	+16 kW	55	SG3	+15 kW
36	L_890	+15 kW	57	SG3	+15 kW
36	SG4	+15 kW	59	SG3	+20 kW

+: Increased power output/withdraw for generator/load;
−: Decreased power output/withdraw for generator/load;
L_890: Load of microgrid 1.

and current waveforms in Fig. 5(a) and Fig. 5(b) show good power quality of the MV distribution system network. The differences in current magnitude across the three phases are results of unbalanced network loads.

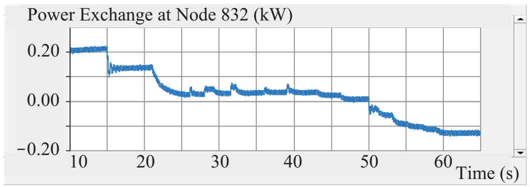

(a)

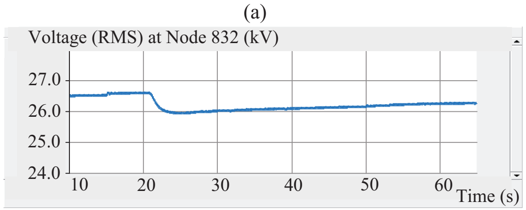

(b)

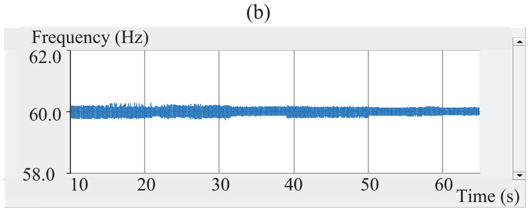

(c)

Fig. 4. Active power (MW), voltage (kV) and frequency (HZ) at microgrid community PCC. (a) Active Power. (b) Voltage. (c) Frequency.

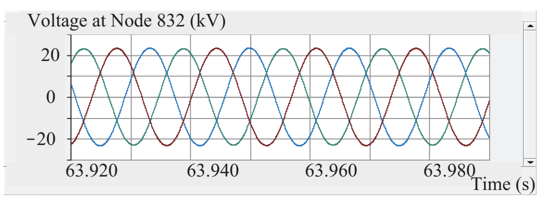

(a)

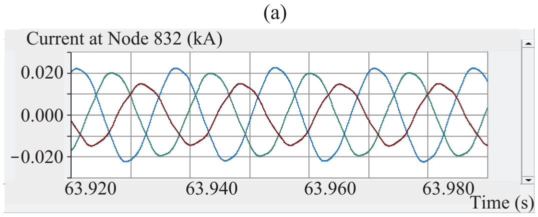

(b)

Fig. 5. Voltage and current waveforms at microgrid community PCC. (a) Voltage. (b) Current.

2) Microgrid A: Fig. 6 shows the active power interchange (exporting) and voltage RMS value at PCC. Fig. 7 shows samples of the steady-state voltage and current waveforms at PCC. Fig. 8 exhibits the steady-state output current waveforms of wind turbine 1 (IG), wind turbine 2 (DFIG), and solar PV. With wind turbine 1 and solar PV, moderate high-order harmonic components are visibly present in the waveforms.

3) Microgrid B: The active power interchange and voltage profile at the PCC during the economic dispatch are shown in Fig. 9. Samples of the PCC steady-state voltage and current waveforms are shown in Fig. 10 where high order-harmonic content is presented in voltage due to onsite solar PV generation.

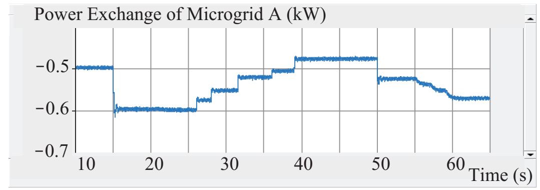

(a)

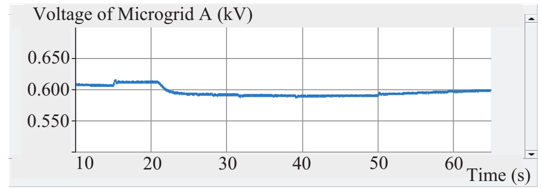

(b)

Fig. 6. Active power and voltage of microgrid A. (a) Active power interchange (negative MW for exporting). (b) Voltage.

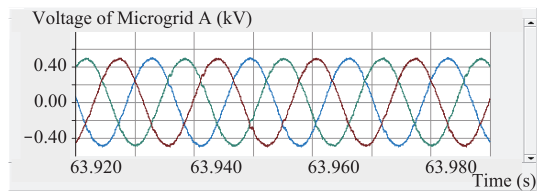

(a)

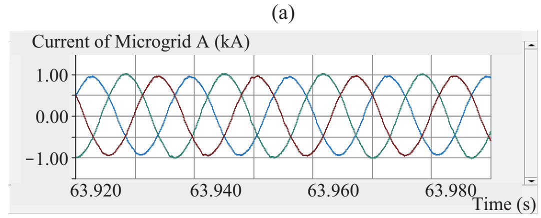

(b)

Fig. 7. PCC voltage and current waveforms of microgrid A. (a) Voltage. (b) Current.

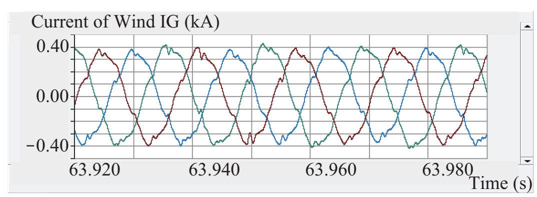

(a)

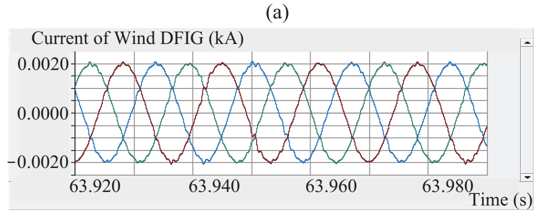

(b)

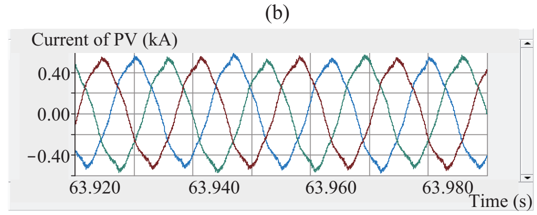

(c)

Fig. 8. Wind and solar PV current output waveforms in Microgrid A. (a) Wind (IG). (b) Wind (DFIG). (c) Solar PV.

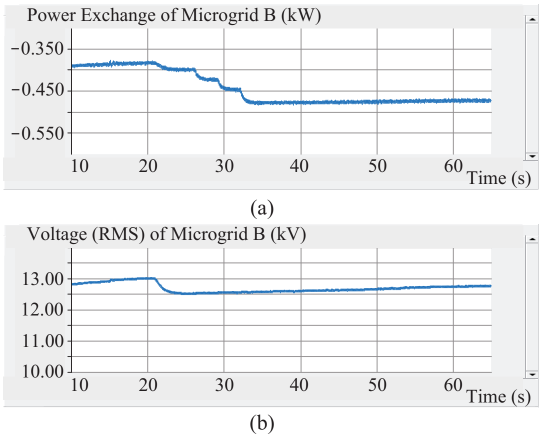

Fig. 9. PCC active power and voltage of microgrid B. (a) Active power interchange (negative MW for exporting). (b) Voltage.

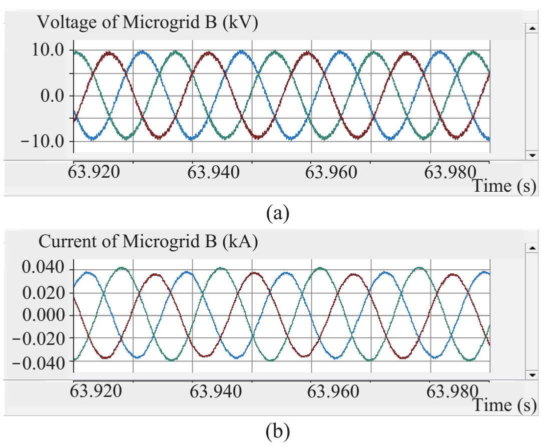

Fig. 10. PCC voltage and current waveforms of microgrid B. (a) Voltage. (b) Current.

4) Microgrid C: The active power interchange and voltage profile at the PCC, as well as the PCC steady-state voltage and current waveforms are shown in Fig. 11 and Fig. 12, respectively. It is also noted that the quick ramp of BESS active power at $t = 15$ s creates transients across the microgrid community, as shown in Fig. 13.

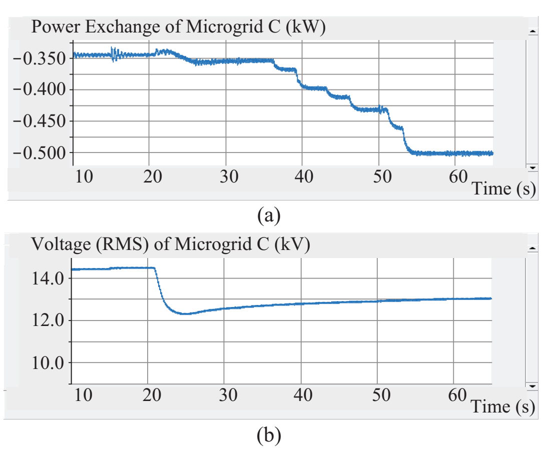

Fig. 11. PCC active and of microgrid C. (a) Active power interchange (negative MW for exporting). (b) Voltage (kV).

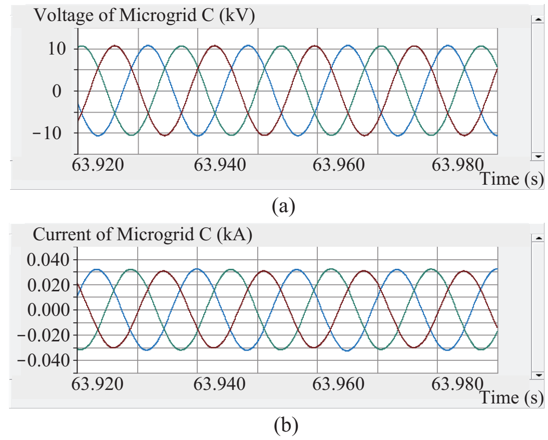

Fig. 12. PCC voltage and current waveforms of microgrid C. (a) Voltage. (b) Current.

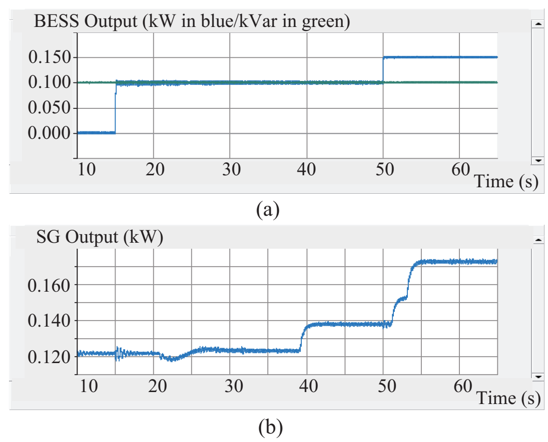

Fig. 13. BESS deployment (microgrid A) at $t = 15$ s and SG6 active power transient (microgrid C) (ripples around $t = 15$ s). (a) BESS. (b) SG6.

B. Discussion

Throughout the active power economic dispatch, the microgrid community is able to maintain voltage and frequency stabilities as the generator outputs vary drastically. The following key observations are from the simulation case study:

1) Distributed generation power is mostly consumed locally by microgrid loads or by network loads that are close to the microgrid PCC, avoiding long distance power transmission between buses that are connected with generation sources. The dynamic interactions among the voltage regulation controls of distributed generation resources are damped by the nearby voltage-dependent loads, resulting in weaker coupling among the generation resources. This network operation feature has positive impact on voltage stability in distribution systems where the distributed generation resources actively perform voltage regulation based on local voltage measurements.
2) In the grid connected mode of operation, the P-f droop control and Q-V droop control of a distribution generation resource are decoupled from each other, since frequency f reflects the bulk power system frequency

and is not affected by local voltage and load changes.

3) The Q-V droop parameters of synchronous generators are critical to the network stability. High values of droop response R cause the system to be prone to voltage instability. In addition, the excitation voltage PI control must be on slower time scale than the turbine governor P-f droop control, with reduced gain and time constant.
4) The ramping of power electronically interfaced generation resources, such as a BESS unit through smart inverter is very fast. Therefore, the magnitude of active power change (increase or decrease) per ramping action should be limited, to avoid creating undesirable voltage and current transients in the network.

IV. Islanded Operation

The microgrid community can operate in the islanded mode as a result of intentional islanding or unintentional islanding. Mitigating voltage and current transients are primary challenges for the transition process from grid-connected to islanded mode. It is particularly more challenging for unintentional islanding as it involves quick power outage detection and deployment of fast response generation resources such as batteries and diesel units following the power outage. Successful transitions depend on both effective deployment of the hardware equipment involved and microgrid operating conditions prior to islanding. There have been many discussions in the research literature on the strategies for unintentional islanding and blackstart of microgrids [17]. The islanding strategy for a community of multiple microgrids is a separate study topic by itself and will not be elaborated here. In the following simulation study, intentional islanding takes place where the microgrid community has dispatched adequate generation to meet its local load demand before islanding took place.

A. Intentional Islanding

Prior to islanding, the microgrid community was serving all of its local demand by distributed generation. Therefore, the active power interchange at the microgrid community PCC is nearly zero. The reactive power interchange is 90 kVar exporting. Fig. 14 shows the voltage and frequency around the time ($t = 15$ s) when the PCC switch is opened. No significant transients are seen to be present in either voltage or frequency.

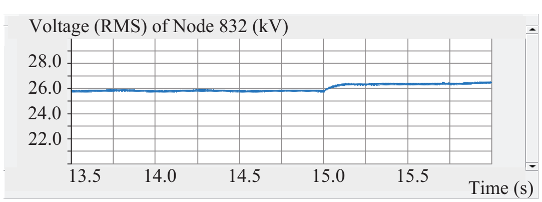

(a)

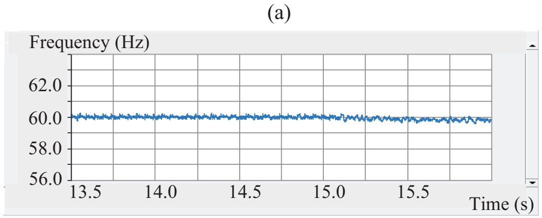

(b)

Fig. 14. Voltage and frequency at microgrid community PCC before and after microgrid islanding (at $t = 15$ s). (a) Voltage. (b) Frequency.

B. Steady State Operation

The essential challenges for the islanded operation of the microgrid community are frequency and voltage regulations through effective primary and secondary controls. With the primary droop controls described in section II C, all synchronous generation units are placed on the P-Q control mode with both P-f and Q-V droops. The economic dispatch of the microgrid community is expected to send active and reactive power setpoints to the microgrid community to manage voltage and frequency excursions from their nominal levels, in a manner similar to the AGC (automatic generation control) function of bulk power system operation. In addition, there must be ample contingency reserves (P_{res}, Q_{res}) procured by the microgrids so that the microgrid community can ensure both frequency and voltage security of the islanded distribution system network if unexpected events occur, such as abrupt changes in load, generation and network topology. With the absence of such secondary control functions, this study will mainly examine the voltage and frequency stabilities after the microgrid community has become islanded. Both small and large disturbance events are emulated while the voltages and currents are monitored at key nodal locations.

1) Steady-State Voltages and Currents: Table II shows the steady state voltages in per unit RMS values. Figs. 15, 16, and 17 show the steady-state voltage and current waveforms at the PCC of the microgrids A, B, and C. Fig. 18 shows the steady-state output current waveforms of inverter-based distributed generation resources. The waveforms show various

TABLE II
Voltage per Unit Value at Each Node of MGC

Node	Voltage	Node	Voltage	Node	Voltage
832	0.9946	834	0.9955	860	0.9961
858	0.9949	842	0.9963	836	0.9959
864	0.9949	844	0.9966	840	0.9958
888	0.9845	846	0.9968	838	0.9210
890	0.9618	848	0.9968	862	0.9959

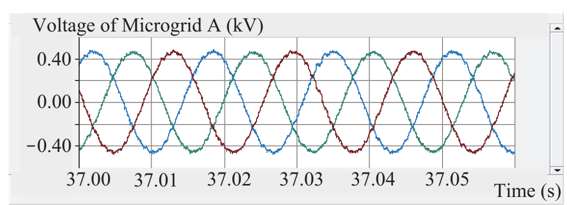

(a)

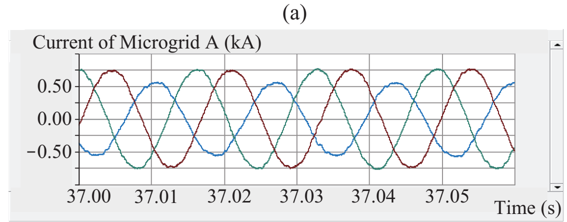

(b)

Fig. 15. PCC voltage and current waveforms of Microgrid A. (a) Voltage. (b) Current.

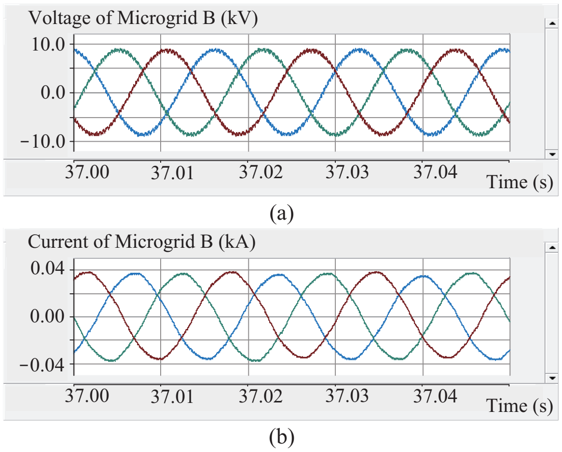

Fig. 16. PCC voltage and current waveforms of Microgrid B. (a) Voltage. (b) Current.

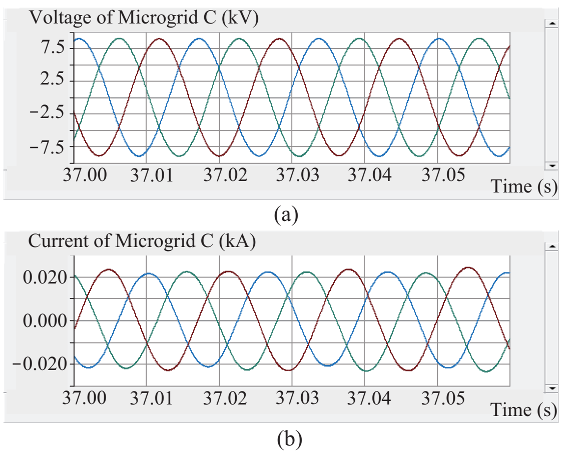

Fig. 17. PCC voltage and current waveforms of microgrid C. (a) Voltage. (b) Current.

degree harmonic distortions (especially of high orders) in the inverter output currents, more visible than when the microgrid community is operating in the grid-connected mode. The waveforms show slight high-order harmonic distortions. Fig. 19 shows the Fast Fourier Transformation (FFT) analysis of the voltages and currents at the PCCs of the microgrids and the microgrid community.

2) Small Disturbance Stabilities: A series of small disturbances is emulated for the islanded microgrid community as shown in Table III. Fig. 20 shows the voltage and frequency response during the disturbances. It shows that although voltage and frequency stabilities are maintained throughout the events, the excursions can travel outside the normal ranges.

TABLE III
TIMES AND SCALES OF SMALL DISTURBANCE EVENTS

T (s)	Device	ΔP, ΔQ	T (s)	Device	ΔP, ΔQ
20	L_890	−20 kW	30	SGs 1, 2	24 kW
23	SGs 5, 6	20 kW	37	Solar_844	−20 kW
28	L_860	−24 kW	37	Load_860	−20 kVA

L_890: Load inside microgrid A (with PCC at node 890).
Solar_844: Solar PV inside microgrid B (with PCC at node 844).

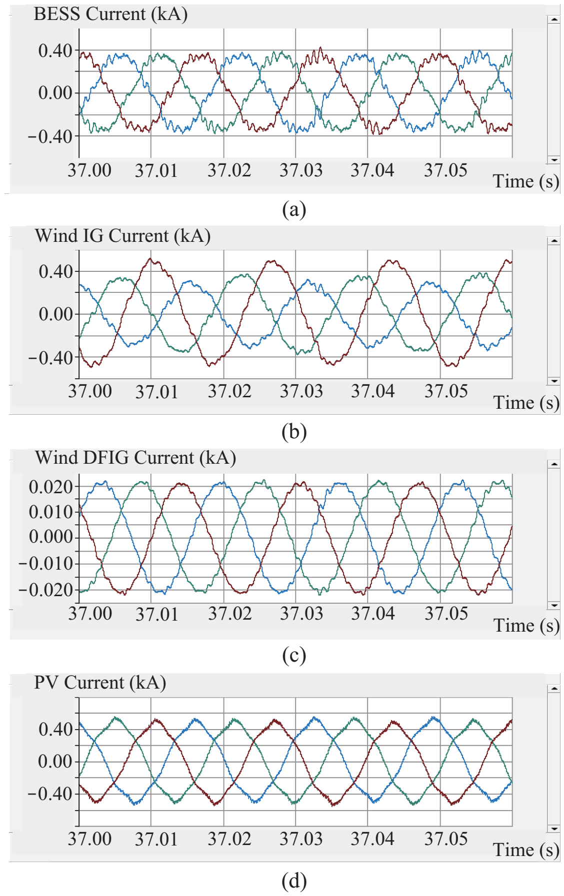

Fig. 18. Renewable distributed generation output current in microgrid A. (a) BESS. (b) Wind (IG). (c) Wind (DFIG). (d) Solar PV.

Corresponding secondary controls must be deployed on time to adjust generation setpoints to steer frequency and voltage to within the security ranges (e.g., 59.5–60.5 Hz for frequency and 0.95–1.05 p.u. for voltage [6]), to prevent equipment damage from prolonged voltage and frequency excursions. In this study, the BESS in microgrid A was deployed to generate 330 kVar reactive power at $t = 22$ s, recovering the sagging system voltage across the microgrid community (Fig. 20).

3) Stability After a Three-Phase Ground Fault: A three phase ground fault was set to occur at $t = 40$ s at node 832 (microgrid community PCC) and cleared after 0.1 second. The system voltage recovered after the fault cleared. Severe oscillation persisted for a long time period, as shown in Fig. 21(a). Even after the fault clearing time was changed to 0.05 s, the voltage oscillation persisted (Fig. 21(b)).

C. Discussion

This simulation case study has shown the feasibility of operating the microgrid community in the islanded mode. There are the following important observations from this case study.

1) A primary control mechanism is not necessarily required for carrying out a planned islanding process by managing the power interchange at the PCC to be precisely at zero levels. As long as the PCC power interchange is

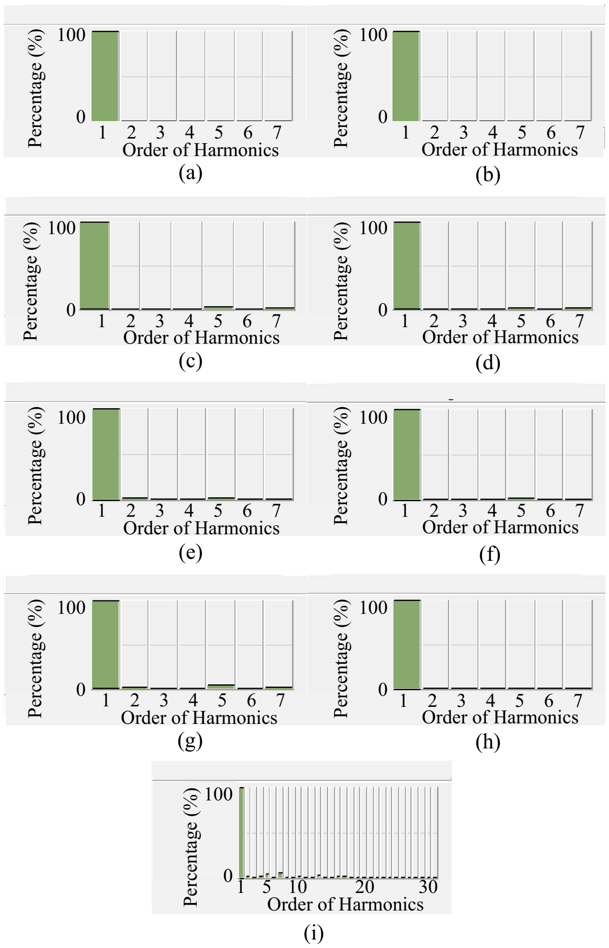

Fig. 19. FFT analysis of voltage and current waveforms at the microgrid PCCs. (a) and (b) Voltage and current FFT of microgrid A. (c) and (d) Voltage and current FFT of microgrid B. (e) and (f) Voltage and current FFT of microgrid C. (g) and (h) Voltage and current FFT at node 852. (i) Current FFT of BESS in microgrid A.

held at low enough levels through a secondary control function (such as the economic dispatch), operational mode transition can take place without significant voltage transients. In this case, the dynamic impacts on the microgrid community are similar to that of a small disturbance, such as the loss of a small generation unit or load.

2) The P-f and Q-V droop controls of the generation resources are coupled during the islanded mode of operation due to the high R/X ratio of distribution lines and voltage dependent loads. It is essential that the coupling should not lead to system voltage and frequency instability. This simulation shows that with well-adjusted droop control constants, the distribution system operation can quickly settle at new equilibrium points.

3) Robust system stability can be achieved through the primary droop controls during small disturbance events, such as normal synchronous generator output ramping and abrupt load changes. The Q-V linear droop constant R of synchronous generators must be kept at low enough levels. Otherwise, significant voltage oscillations will occur.

4) Due to the relative small scale of the islanded microgrid community system, the steady-state voltage and frequency can easily travel outside their normal ranges due to changes in system operating conditions. This calls for more frequent deployment of secondary control functions to adjust generation setpoints in order to restore voltage and frequency to safety levels. Also, the system stability is more susceptible to faults. Addition primary controls would be required to attenuate post-fault voltage and current oscillations in the system.

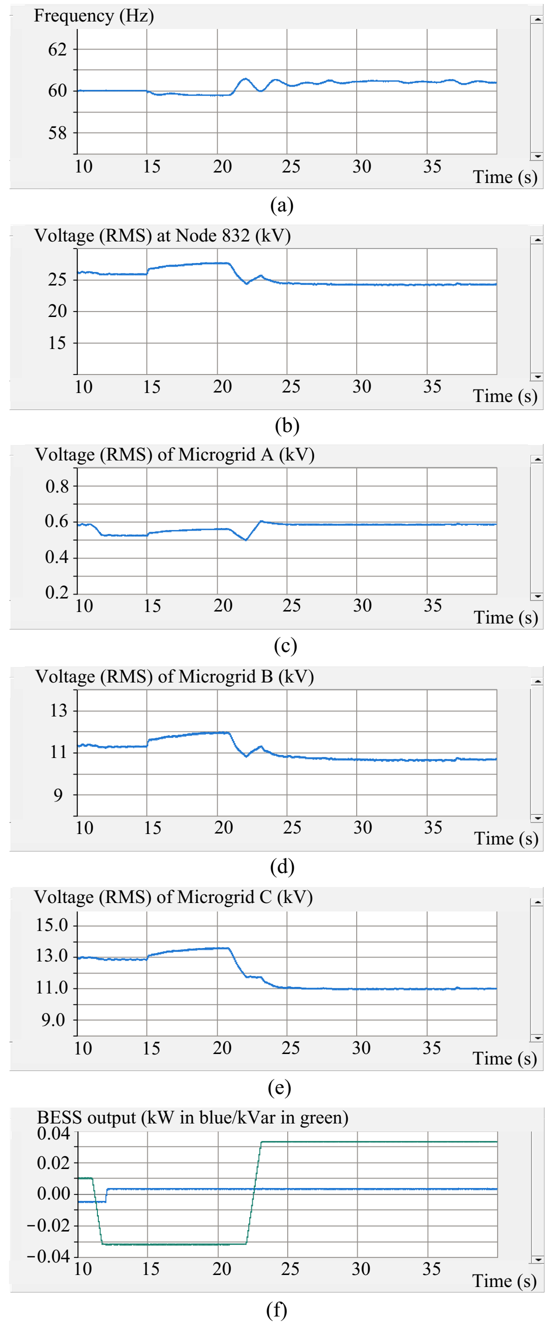

Fig. 20. System frequency and microgrid PCC voltages (in kV) during small disturbance events; and microgrid A BESS real and reactive power deployment. (a) Frequency. (b) Voltage at 832. (c) Voltage at 890. (d) Voltage at 844. (e) Voltage at 860. (f) BESS deployment.

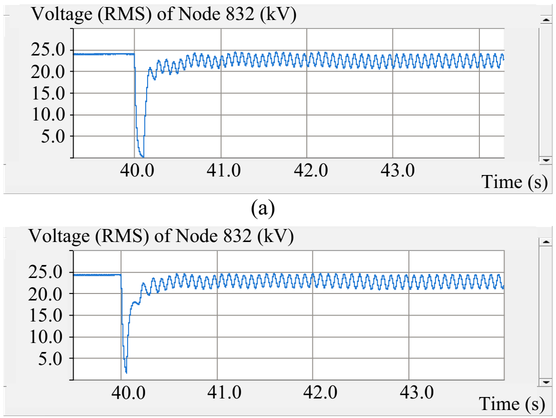

(b)

Fig. 21. Microgrid community PCC voltage during fault. (a) Tclr = 0.1 sec. (b) Tclr = 0.05 s.

V. Conclusion

This study has constructed a detailed PSCAD electromagnetic model for the study of a microgrid community that involves three microgrids networked through the MV distribution system. A number of typical operational scenarios are simulated, including economic dispatch, load changes, voltage events, operational mode transition, and small and large network disturbances in the islanded mode. The simulation case studies have shown the operational feasibility of networked microgrids in electrical distribution systems, and the effectiveness of P-Q based primary controls with droop characteristics in facilitating energy transaction of the microgrids and maintaining voltage and frequency stabilities under normal network disturbances. The future work will focus on deriving secondary and tertiary controls for computing primary control setpoints to achieve both economic objectives and operational security requirements.

(Due to presentation limits, some parameters used in the simulation are not shown here, but they will be made available upon any inquiries.)

References

[1] R. Lesseter, "MicroGrids," in *IEEE Power Engineering Society Winter Meeting 2002*, vol. *1*, 2002, pp. 305–308.
[2] N. Hatziagyriou, H. Asano, R. Iravani, and C. Marnay, "Microgrids," *IEEE Power and Energy Magazine*, vol. 5, no. 4, pp. 78–94, 2007.
[3] G. Strbac, N. Hatziargyriou, J. P. Lopes, C. Moreira, A. Dimeas, and D. Papadaskalopoulos, "Microgrids: Enhancing the resilience of the European megagrid," *IEEE Power and Energy Magazine*, vol. 14, no. 3, pp. 35–43, 2015.
[4] M. Smith and D. Ton, "Key Connections: the U.S. Department of Energy's microgrid initiative," *IEEE Power and Energy Magazine*, vol. 11, no. 4, pp. 22–27, 2013.
[5] M. Montoya, R. Sherick, P. Haralson, R. Neal, and R. Yinger, "Island in the storm: integrating microgrids into the larger grid", *IEEE Power and Energy Magazine*, vol. 11, no. 4, pp. 33–39, July 2013.
[6] *IEEE Guide for Design, Operation, and Integration of Distributed Resource Island Systems with Electric Power Systems*, IEEE Standard 1547.4, 2011.
[7] "Microgrid study: Energy security for DoD installation," MIT Lincoln Lab Report, 2012.
[8] Microgrid at Illinois Institute of Technology. [Online]. Available: http://www.iitmicrogrid.net/.
[9] N. Hatziargyriou, "The more microgrids project," in *Smart Electricity Networks,* retrieved from Demonstration of Smart Distribution Network Solutions, Contractors Meeting, Brussels, Sep. 2009. Available: https://ec.europa.eu/research/conferences/2009/smart_networks/pdf/microgrids.pdf
[10] A. Bidram and A. Davoudi, "Hierarchical structure of microgrids control system," *IEEE Transactions on Smart Grid*, vol. 3, no. 4, pp. 1963–1976, May 2012.
[11] M. Yazdanian and A. Mdhrizi-Sani, "Distributed control techniques in microgrids," *IEEE Transactions on Smart Grid*, vol. 5, no. 6, pp. 2901–2909, Nov 2014.
[12] H. Han, X. Hou, J. Yang, J. Wu, M. Su, and J. M. Guerrero, "Review of power sharing control strategies for islanding operation of AC microgrids," *IEEE Transactions on Smart Grid*, vol. pp., no. 99, pp. 1,1 10.1109/TSG.2015.2434849.
[13] A. K. Marvasti, Y. Fu, S. DorMohammadi, and M. Rais-Rohani, "Optimal operation of active distribution grids: a system of systems framework," *IEEE Transactions on Smart Grid*, vol. 5, no. 3, pp. 1228–1237, May 2014.
[14] L. Che, M. Shadidehpour, A. Alabdulwahab, and U. Al-Turki, "Hierarchical coordination of a community microgrid with AC and DC microgrids," *IEEE Transactions on Smart Grid*, vol. 6, no. 6, pp. 3042-3051, Nov 2015.
[15] Z. Wang, B. Chen, J. Wang, and C. Chen, "Networked microgrids for self-healing power systems," *IEEE Transactions on Smart Grid*, vol: pp, no. 99, pp. 1, 10.1109/TSG.2015.2427513.
[16] Q. Fu, L. F. Montoya, A. Solanki, A. Nasiri, V. Bhavaraju, T. Abdallah, and D. C. Yu, "Microgrid generation capacity design with renewable and energy storage addressing power quality and surety," *IEEE Transactions on Smart Grid*, vol. 3, no. 4, pp. 2019–2027, Dec 2012.
[17] Q. Fu, A. Nasir. V. Bhavaraju, A. Solanki, T. Abdallah, and D. C. Yu, "Transition management of microgrids with high penetration of renewable energy," *IEEE Transactions on Smart Grid,* vol. 5, no. 2, pp. 539–549, Mar. 2014.
[18] PSCAD, Manitoba Hydro International Ltd. https://hvdc.ca/pscad/
[19] IEEE PES Distribution Analysis Subcommittee Radial Test Feeders, http://ewh.ieee.org/soc/pes/dsacom/testfeeders/

Fan Zhang (S'14) is currently pursuing her Master's degree in the Department of Electrical Engineering and Computer Science, Case Western Reserve University. She received her B.S. in power systems in Hunan University of China in 2013. Her current research interests include power system analysis, control of microgrids and stochastic programming.

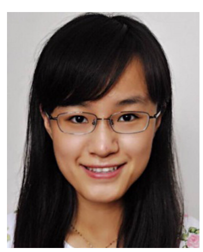

Huiying Zhao (S'15) is currently pursuing her Ph.D. degree in the Department of Electrical Engineering and Computer Science, Case Western Reserve University. She received her B.S. and M.S. degree in power systems from Tianjin University of China in 2011 and 2014 respectively. Her current research interests include controls and simulation of microgrid, and smart grid engineering.

Mingguo Hong (S'93–M'98) received his B.E. degree in electrical engineering from Tsinghua University in 1991, M.S. degree in Mathematics from the University of Minnesota in 1993 and Ph.D. degree in electrical engineering from the University of Washington in 1998. He worked as a power systems engineer at ALSTOM Grid in Redmond, Washington from 1998 to 2005, an Associate Professor of Mathematics at Valley Forge Military College from 2005 to 2006, and a principle market engineer at the Mid-continent Independent System Operator (MISO) in Carmel, Indiana from 2006 to 2012. He is currently an Associate Professor in the Electrical Engineering and Computer Science department of the Case Western Reserve University in Cleveland, Ohio. His research interests are in power system analysis, electricity markets and smart distribution systems.